A Wavelet-based Feature Extraction with Dynamic Time Warping Alignment for Real-Time Fire Detection based on Streaming Sensor Data

Hosung Lee

Department of Industrial and Systems Engineering

Rutgers, The State University of New Jersey

2021. 5.

Contents

Part 1: Motivation

1.1 Motivation

- Fire accidents are one of the most catastrophic threats to cause human injuries and fatalities compared to other disasters
  - According to International Association of Fire and Rescue Services, fire hazards have caused 16,190 casualties between 2012 and 2016 in the US (Gaur et al., 2019)

- False alarms are a major concern of existing fire monitoring methods
  - Cause needless evacuation and emergency plans
  - Economical loss from the false alarm in the aircraft is estimated to cost between $30,000 and $50,000 (Chen et al., 2007)

- Necessity of reliable, and accurate fire detectors
  - Reduce the loss of lives and infrastructure damages
  - Reduce financial losses and panic

1.2 Fire disaster and building automation

- Building fire is mostly caused mainly by human inaction
- Generally heat, smoke and flame occurs when fire ignites
- Major causes for building fire are:
- Com
  - Cooking
  - Heating equipment
  - Smoking
  - Electrical equipment

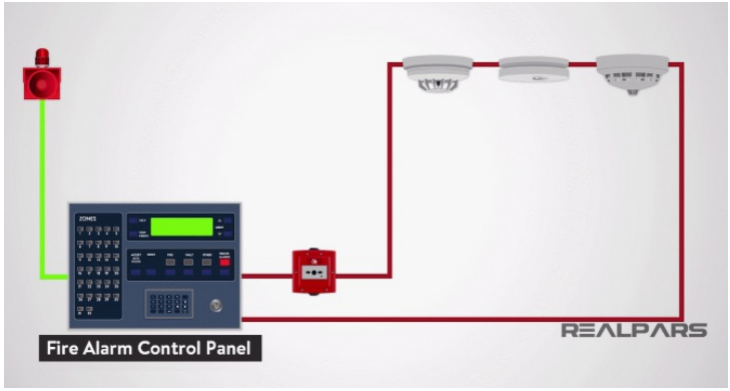

- **Fire detector with novel detection algorithm connected to SCADA system for automated control**

*Supervisory control and data acquisition (SCADA) is a control system architecture comprising computers, networked data c ommunications and graphical user interfaces (GUI) for high-level process supervisory management,

*RS-485/Modbus communication protocol

Source: https://en.wikipedia.org/wiki/Structure_fire

Part 2:
Fire Data

2.1 Overview of Collected Data

- Objective
  - Response of fire monitoring sensors to different residential fire setting scenarios
- Following sensors are used to collect the data
  - Temperature sensor
  - CO sensor
  - Ionization sensor
  - Photoelectric sensor
  - Smoke obscuration sensor
- Following data are collected over time
  - Temperature
  - CO
  - Smoke obscuration level

Source: Bukowski, R. W., Peacock, R. D., Averill, J. D., Cleary, T. G., Bryner, N. P., & Reneke, P. A. (2008). Performance of Home Smoke Alarms, Analysis of the Response of Several Available Technologies in Residential Fire Settings (No. Technical Note (NIST TN)-1455-1).

2.2 Data Collection

- Fire generation scenario based on the combination of
  - Type of fire
    - Flaming: A fire that has visible flames and generate high heat
    - Heating: A fire that usually involves cooking oil, medium flames and medium heat
    - Smoldering: A fire that involved slow combustion, invisible flames, low heat, and high sm oke
  - Materials (sofa, mattress, pan)
  - Ignition places (bedroom, living room, kitchen)

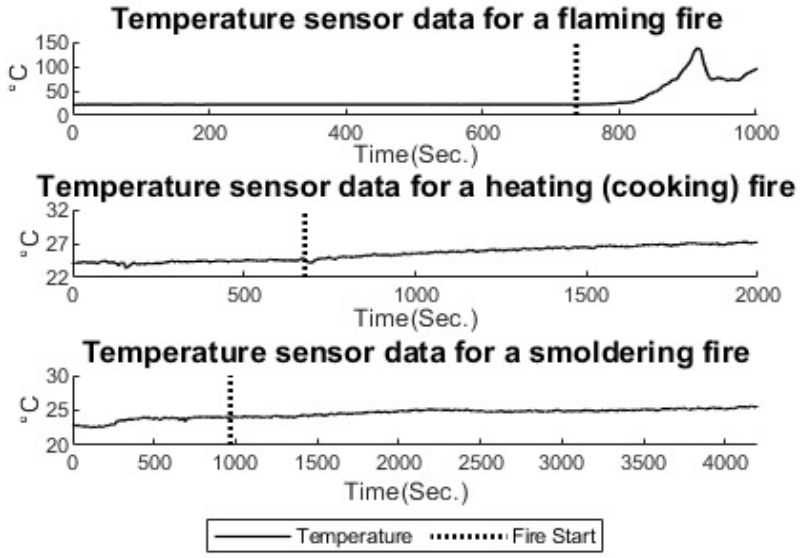

Figure. Behavior of temperature sensor si gnals for different types of fire

2.2 Data Collection

- Testbed setup
  - **One story manufactured home**
- Locations of sensors(3 location)
  - Main bedroom
  - Living room
  - Hallway
- Sensor types(5 sensors)
  - Temperature sensor
  - CO sensor
  - Ionization sensor
  - Photoelectric sensor
  - Smoke obscuration sens

Figure. One story manufactured home

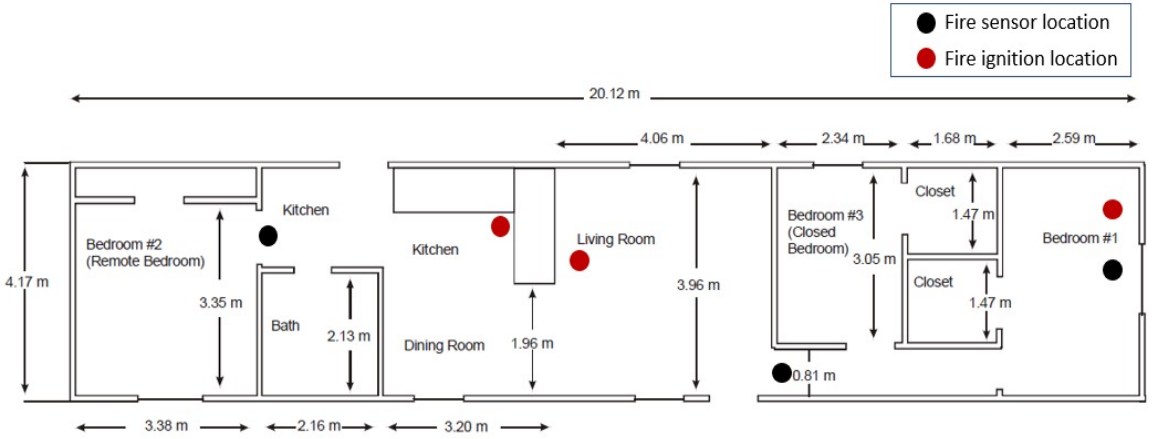

Figure. Layout of manufactured home used for test

15 sensor data

2.2 Data Collection

- For the fire scenarios, a total of 10 fire scenarios under different types of fire were considered
  - Five experiments (i.e., one was used for training and the others were used for testing) were repeatedly performed
  - Various materials such as newspapers, textiles, sponge, and plastic, etc., were used for the ignition
  - True fire starting time was settled to 300 seconds for all fire scenarios

Table. Description of experiment scenarios obtained through the multi-sensor fusion system

Scenario #	Fire type	Fire ignition material	TFST (sec)
1	Heating	Food	300
2	Flaming	Polyurethane	300
3	Flaming	Newspaper	300
4	Smoldering	Newspaper	300
5	Flaming	Plastic	300
6	Flaming	Sponge	300
7	Flaming	Textile	300
8	Smoldering and flaming	Paper and paper towel	300
9	Flaming	Wooden chopsticks	300
10	Flaming	Wooden piece	300

2.3 Data Description

- Attributes
  - Temperature at different locations (i.e., Bedroom, kitchen, hallway)
  - CO concentration at different locations
  - Smoke obscuration at different locations

Table. Dataset obtained from fire scenario

	Living room					Bedroom					Kitchen				
Time (sec)	temp	CO2	Ion	Pho	SM	temp	CO2	Ion	Pho	SM	temp	CO2	Ion	Pho	SM
0	27.8	-0.14	0.00	0.07	0.00	28.3	-0.08	0.01	0.07	0.00	28	-0.03	-0.01	0.00	0.00
1	27.8	-0.22	0.00	0.07	0.00	28.3	0.03	0.01	0.07	0.00	28	-0.03	-0.01	0.00	0.00
2	27.8	-0.30	0.00	0.07	0.00	28.3	0.14	0.01	0.07	0.00	28	-0.03	-0.01	0.00	0.00
3	27.8	-0.23	0.00	0.07	0.00	28.3	0.01	0.01	0.07	0.00	28	-0.03	-0.01	0.00	0.00
4	27.8	-0.16	0.00	0.07	0.01	28.3	-0.13	0.01	0.07	0.00	28	-0.03	-0.01	0.00	0.00
5	27.8	-0.12	0.00	0.07	0.00	28.3	-0.09	0.01	0.07	0.00	28	-0.03	-0.01	0.00	0.00
6	27.8	-0.08	0.00	0.07	0.00	28.3	-0.05	0.01	0.07	0.00	28	-0.03	-0.01	0.00	0.00
7	27.8	0.21	0.00	0.07	0.00	28.3	-0.04	0.01	0.07	0.00	28	-0.03	-0.01	0.00	0.00
8	27.8	0.50	0.00	0.07	0.00	28.3	-0.02	0.01	0.07	0.00	28	-0.03	-0.01	0.00	0.00
9	27.8	-0.29	0.00	0.07	0.00	28.3	-0.43	0.01	0.07	0.00	28	-0.03	-0.01	0.00	0.00
10	27.8	-1.07	0.00	0.07	0.00	28.3	-0.84	0.01	0.08	0.00	28	-0.03	-0.01	0.00	0.00
11	27.8	-0.70	0.00	0.07	0.00	28.3	-0.72	0.01	0.07	0.00	28	-0.03	-0.01	0.00	0.00
12	27.8	-0.34	0.00	0.07	0.00	28.3	-0.60	0.01	0.07	0.00	28	-0.03	-0.01	0.00	0.00
13	27.8	-0.69	0.00	0.07	0.00	28.3	-0.71	0.01	0.07	0.00	28	-0.03	-0.01	0.00	0.00
14	27.8	-1.04	0.00	0.07	0.00	28.3	-0.82	0.01	0.07	0.00	28	-0.03	-0.01	0.00	0.00

⋮

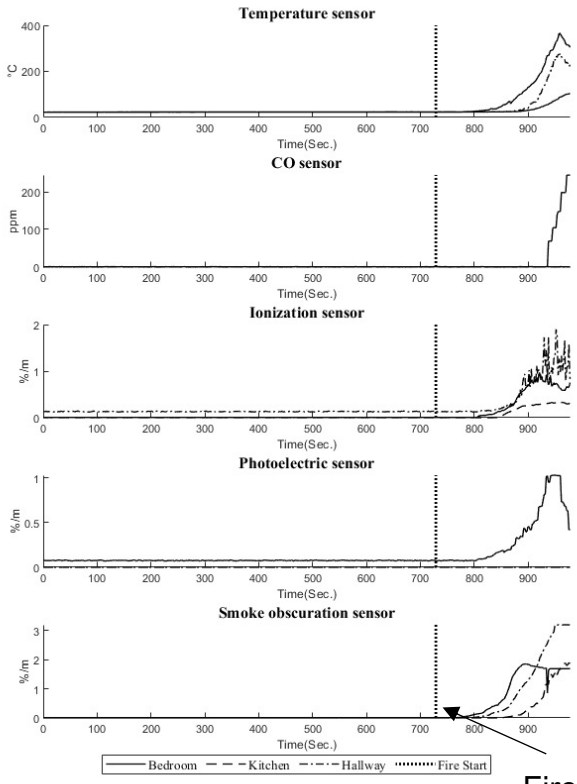

Figure. Signal of a fire scenario 7

2.3 Data Description

- Characteristic of the sensor signals
  - Sensor signals behave differently depending on the **fire type**
    - Smoldering Fire:
      - Photoelectric sensor react faster than ionization
    - Flaming Fire:
      - Ionization sensors react faster than photoelectric

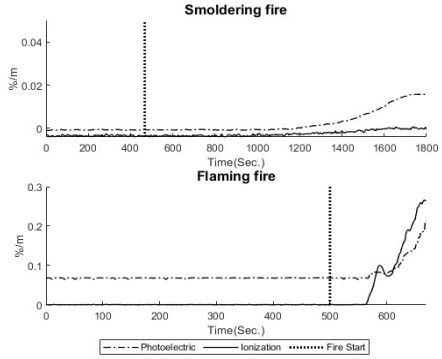

Figure. Temperature signal values of diff erent fire types over time

- Sensors installed near to fire location react faster then locations
  - Sensors near the living room fire (i.e., kitchen an d hallway) rise faster than sensors installed furth er (i.e. bedroom) when the fire occurs in the livi ng room

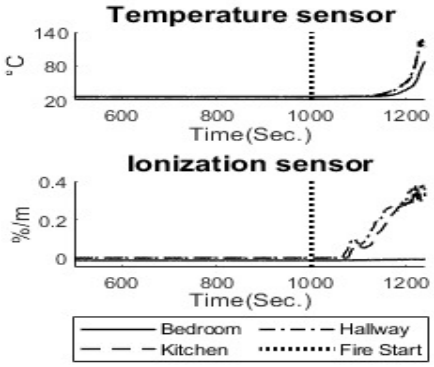

Figure. Behavior of sensor signals when fire ignited in living room

2.3 Data Description

- Flaming scenario
  - Temperature, humidity, CO concentration , and CO2 concentration have a gradual rise
  - O2 concentration decreases rapidly
  - Dust PM1.0 particle measurement has a n incremental spike
  - Dust PM2.5 and dust PM10 have a grad ual increase.
  - Smoke sensors measurements
    - Fluctuate over the whole duration of the sce nario in red and green LEDs
    - IR LED measurement remains constant

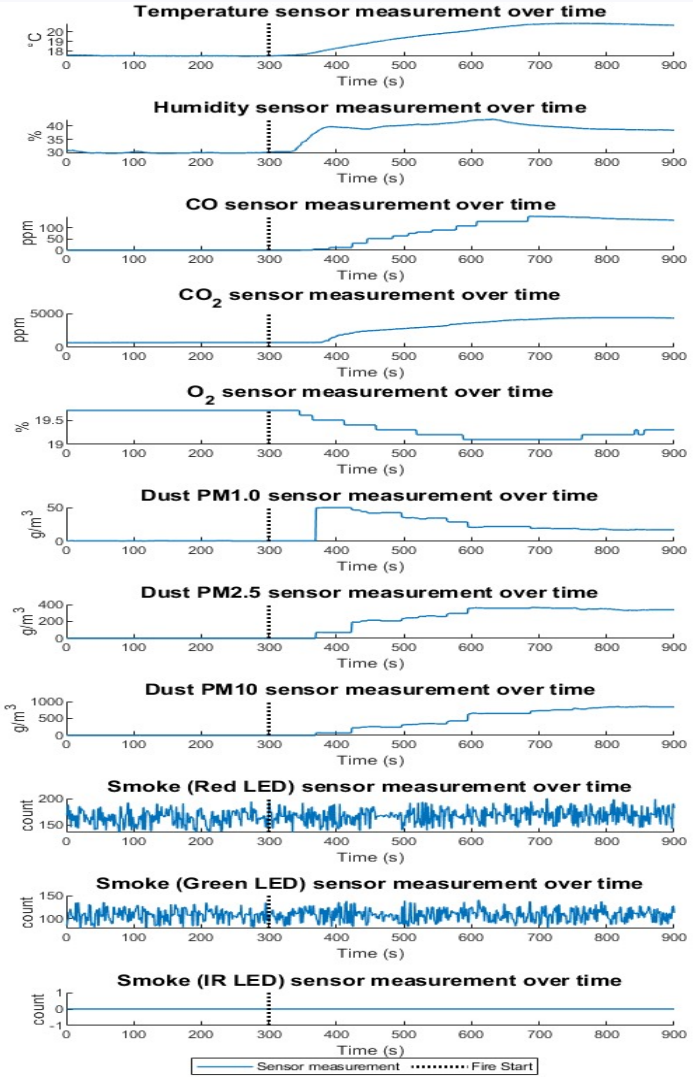

Figure. Recorded sensor signals of all sensors und er smoldering scenario.

2.3 Data Description

- Smoldering scenario
  - Temperature, humidity, CO concentration , and CO2 concentration have a gradual rise
  - O2 concentration remains constant due to low or non-existing flames
  - All dust particles of different diameters r ise rapidly shortly after the fire started
  - Smoke sensors measurements
    - Fluctuate over the whole duration of the sce nario in red and green LEDs
    - IR LED measurement remains constant

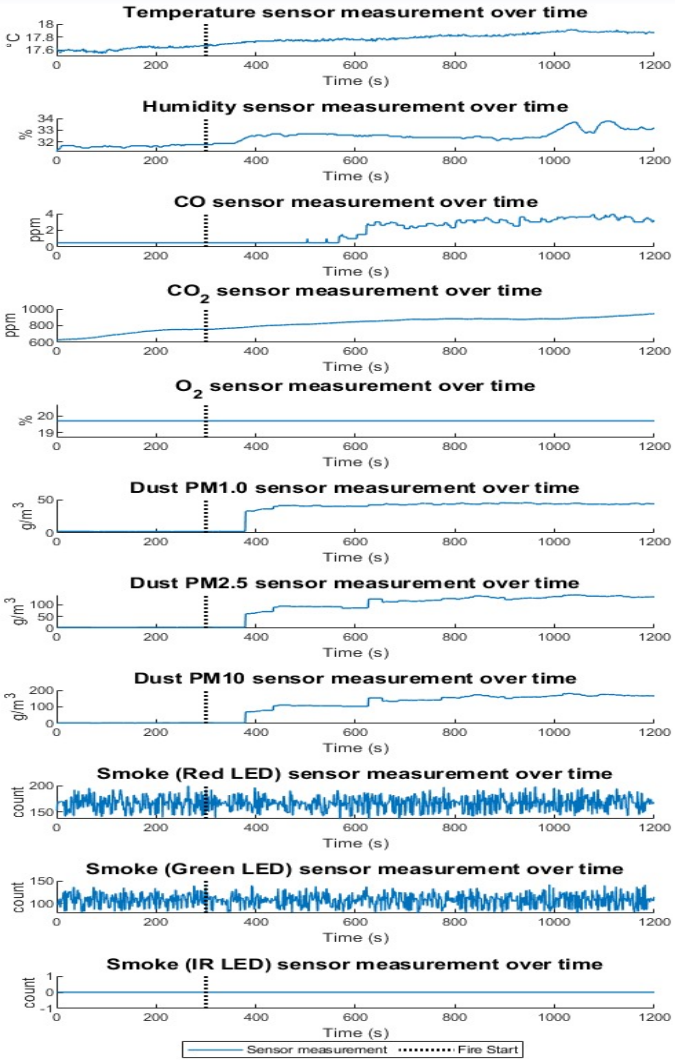

Figure. Recorded sensor signals of all sensors und er smoldering scenario.

2.3 Data Description

- Heating scenario
  - Temperature, humidity, CO2 concentratio n measurements rise gradually
  - CO concentration has a rapid increase
  - O2 concentration has a rapid decrease
    - Not as much as flaming fire scenario
  - Dust PM1.0 particles increase rapidly
  - Dust PM2.5 and dust PM10 increase gra dually
  - Smoke sensors measurements
    - Fluctuate over the whole duration of the sce nario in red and green LEDs
    - IR LED measurement remains constant

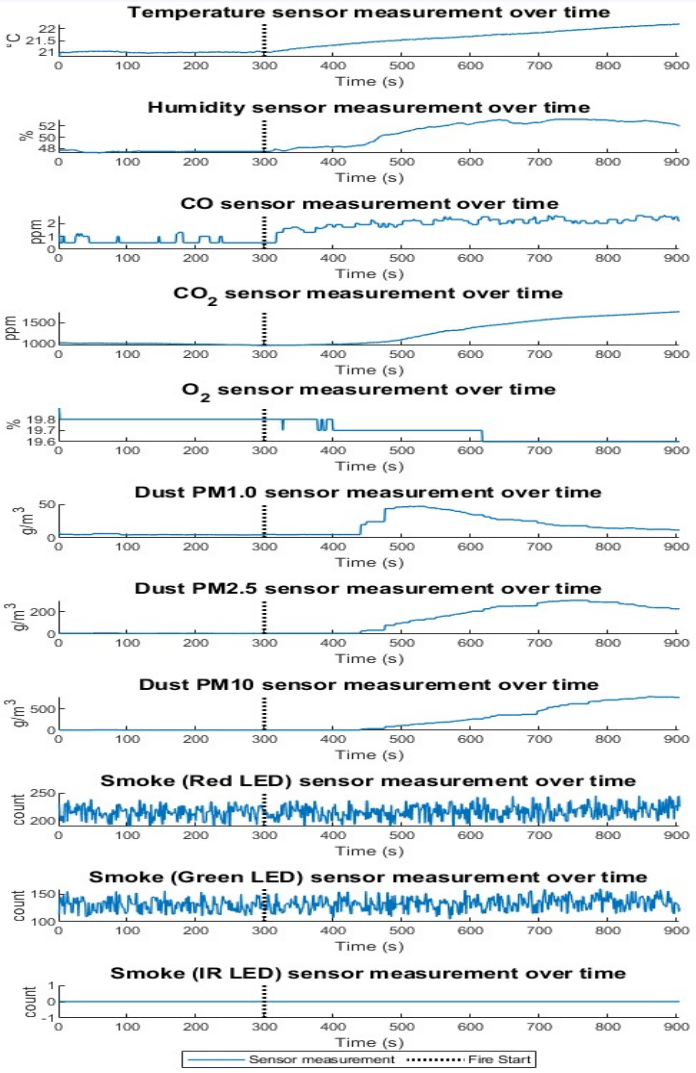

Figure. Recorded sensor signals of all sensors und er heating scenario.

Part 3:
Proposed System

Korea Institute of Science and Technology Information (KISTI)

3.1 Multi-Sensor design for automated detector

- The multi-sensor fusion system consists of three parts:
  - (i) Sensor station
  - (ii) Main station
  - (iii) Data receiver

- Sensor station
  - Six sensor boards
    - Temperature/humidity, CO, CO2, O2, dust, and smoke
- Main station
  - Main board
  - Collect all sensor measurements obtained from sensor boards
  - Transfer collected data to the data receiver
- Data receiver
  - PC-based system
  - Read, save and visualize the sensor data transferred from main station

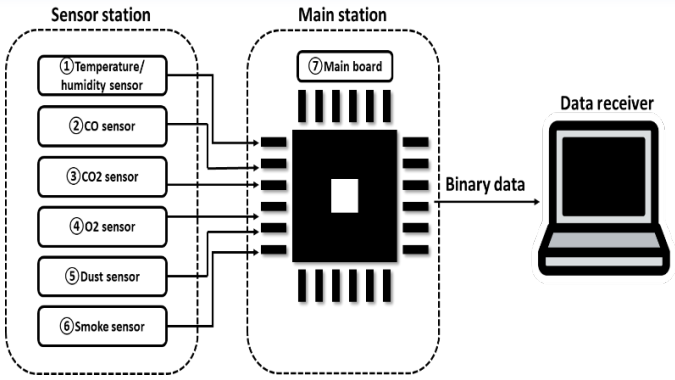

(a)

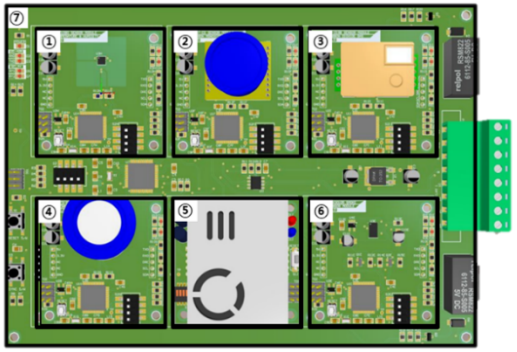

(b)

Figure (a) The conceptual architecture of the multi-sensor fusion system (b) Illustration of th e sensor and main station

3.2 Multi-Sensor (Temperature/ Humidity)

- Temperature and humidity is one of the most critical attributes used in fire detection since
  - Fire generates a high amount of heat through the combustion process which can be measured by temperature sensors
  - Fire humidity also increases rapidly which can help in detecting fires early

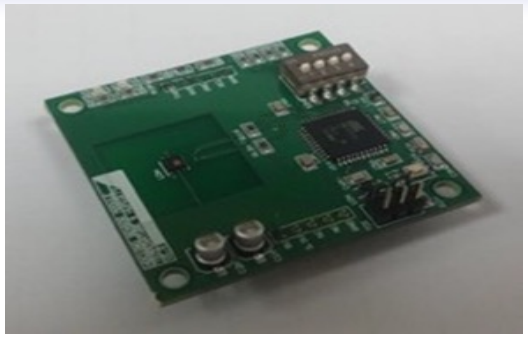

Figure. Illustration of temperature/humidity sensor board (HDC1080)

- Specification of sensor board
  - HDC1080 sensor is used to gather temperature and humidity measurements

Sensor board	Sensor measurement	Measurement range	Measurement accuracy
Temperature / humidity (HDC1080)	Temperature	-40~125 ℃	± 0.2 ℃
	Humidity	0~100 %	± 2 %

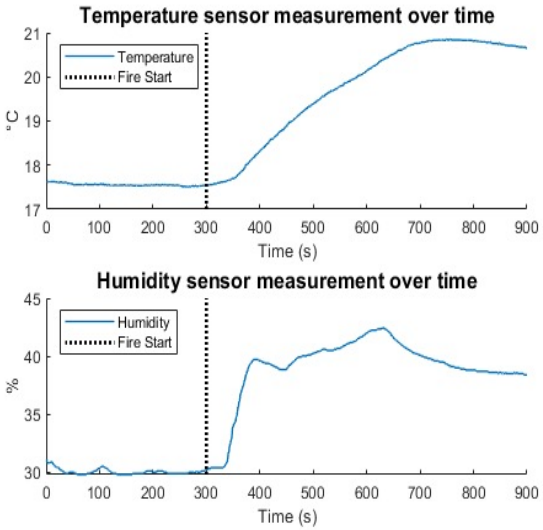

Figure. Reading of temperature and humidity over a fire scenario

- Sensor plot
  - The temperature and humidity measurements rise rapidly after ignition of fire

3.2 Multi-Sensor Sensor Station (CO)

- Fire causes the CO gas concentration to rise rapidly and slowly (depending on the type of fire) over time in others

- Specification of sensor board
  - ZE07-CO sensor is used to gather CO centration in a fire scenario

Sensor boar d	Sensor measurement	Measurement range
CO (ZE07-CO)	CO	0 ~ 500 ppm

- Sensor plot
  - The CO concentration rises rapidly after ignition of fire in this scenario

Figure. Illustration of CO sensor boa rd (ZE07-CO)

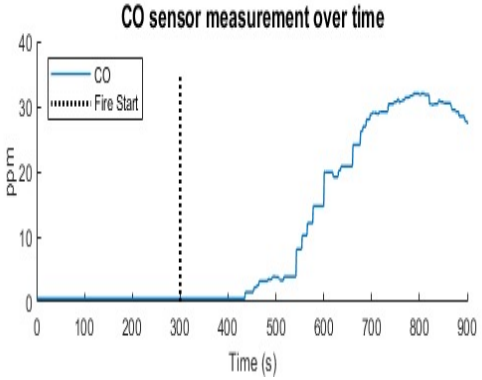

Figure. Reading of CO concentrat ion over a fire scenario

3.2 Multi-Sensor: Sensor Station (O2)

- During fires the O2 concentration in the air decreases, making it of utmost importance in fire detection

Figure. Illustration of O2 sensor boar d (ZE03)

- Specification of sensor board
  - ZE03 sensor is used to gather O2 centration in a fire scenario

Sensor boar d	Sensor measurement	Measurement ran ge	Measurement acc uracy
O2 (ZE03)	O2	0~25%	± 3.5 %

- Sensor plot
  - The O2 concentration decreases after ignition of fire in this scenario due to flames

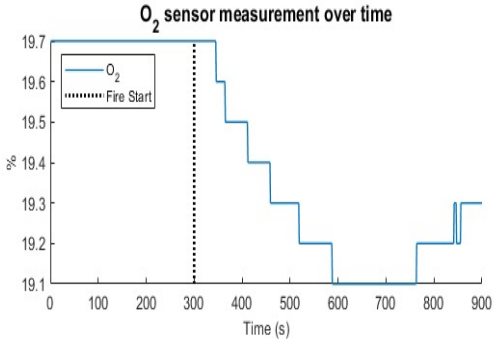

Figure. Reading of O2 concentrati on over a fire scenario

3.2 Multi-Sensor : Sensor Station (Dust)

- Fires generate different particles in the air due to the combustion or burning of ignited items, household, or material.
- Specification of sensor board
  - PMS7003 sensor is used to gather dust centration in a fire scenario
  - Particle diameters ranges are:
    - 0.3-1μm (DUST PM1.0)
    - 1-2.5 μm (DUST PM2.5)
    - 2.5-10 μm (DUST PM10)

Sensor board	Sensor measurement	Measurement range	Measurement accuracy
Dust (PMS 7003)	PM1.0 dust intensity PM2.5 dust intensity PM10 dust intensity	0.0 ~ 500.0ug/m^3	± 10% (100~500µg/m^3), ±10µg/m^3 (0~ 100µg/m^3)

- Sensor plot
  - The dust particles measurement rises
    - Rapidly for Dust PM1.0 particles.
    - Gradually for Dust PM2.5 and Dust PM10 particles

Figure. Illustration of dust sensor board (PMS7003)

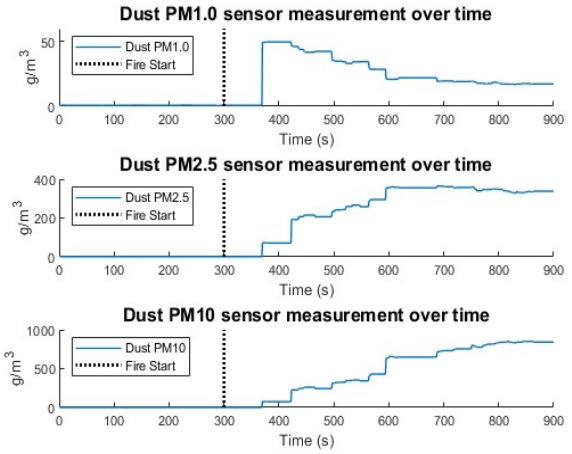

Figure. Reading of dust particles over a fire scenario

3.2 Multi-Sensor : Sensor Station (Smoke)

- Fire produces smoke during the burning and combustion process, but it differs depending on the fire type

- Specification of sensor board
  - MAX30105 sensor is used to gather smoke centration in a fire scenario
  - three light-emitting diodes (LEDs)
    - Red (Red LED)
    - Green (Green LED)
    - Infrared (IR LED)

Sensor board	Sensor measurement	Measurement range
Smoke (MAX30105)	ADC count of red LED ADC count of green LED ADC count of IR ray LED	0~65536 count

- Sensor plot
  - The smoke particles reading keeps fluctuating for red and green LEDs.
  - The smoke particles reading stays constant for IR LED.

Figure. Illustration of smoke sensor board (MAX30105)

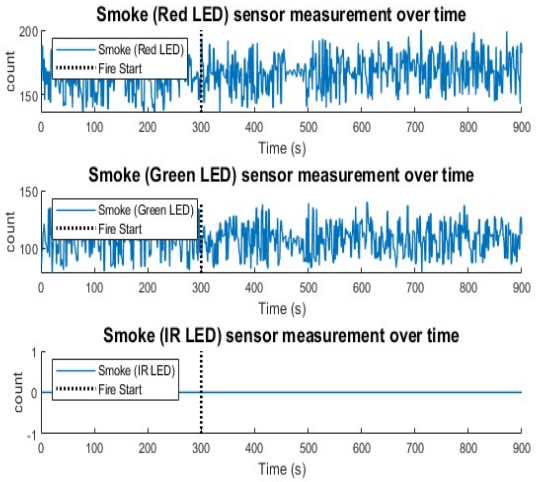

Figure. Reading of smoke particles over a fire scenario

3.2 Multi-Sensor : Main Station (Main Board)

- Main board description
  - The purpose is to collect all sensor measurements obtained from sensor boards and transfer them to the data receiver
  - Consists of several integrated circuit (IC) chips
  - Inter-Integrated Circuit (I^2C) communication system is used to communicate among IC chips
  - The mainboard communicates with an external PC using use the Modbus protocol/RS-485 interface

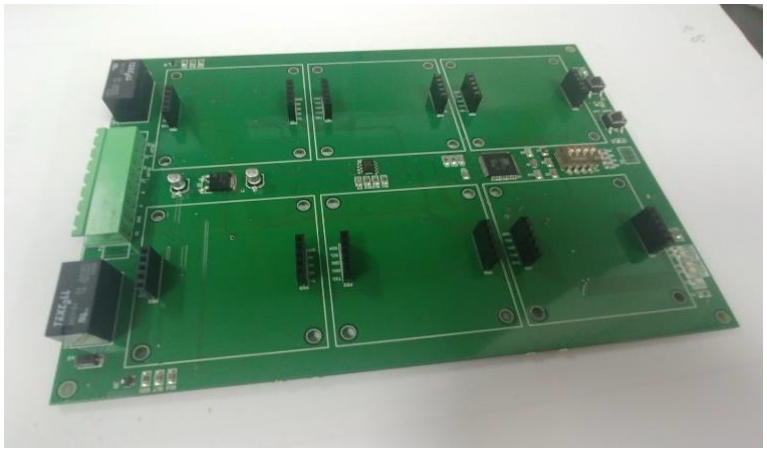

Figure. Illustration of the main board

3.2 Multi-Sensor : Data Receiver

- Data receiver description
  - PC-based system responsible for reading, saving, and visualizing the fire sensor data
  - Modbus protocol is used for delivering the data from contact point to relay(fire extinguisher or alarm)

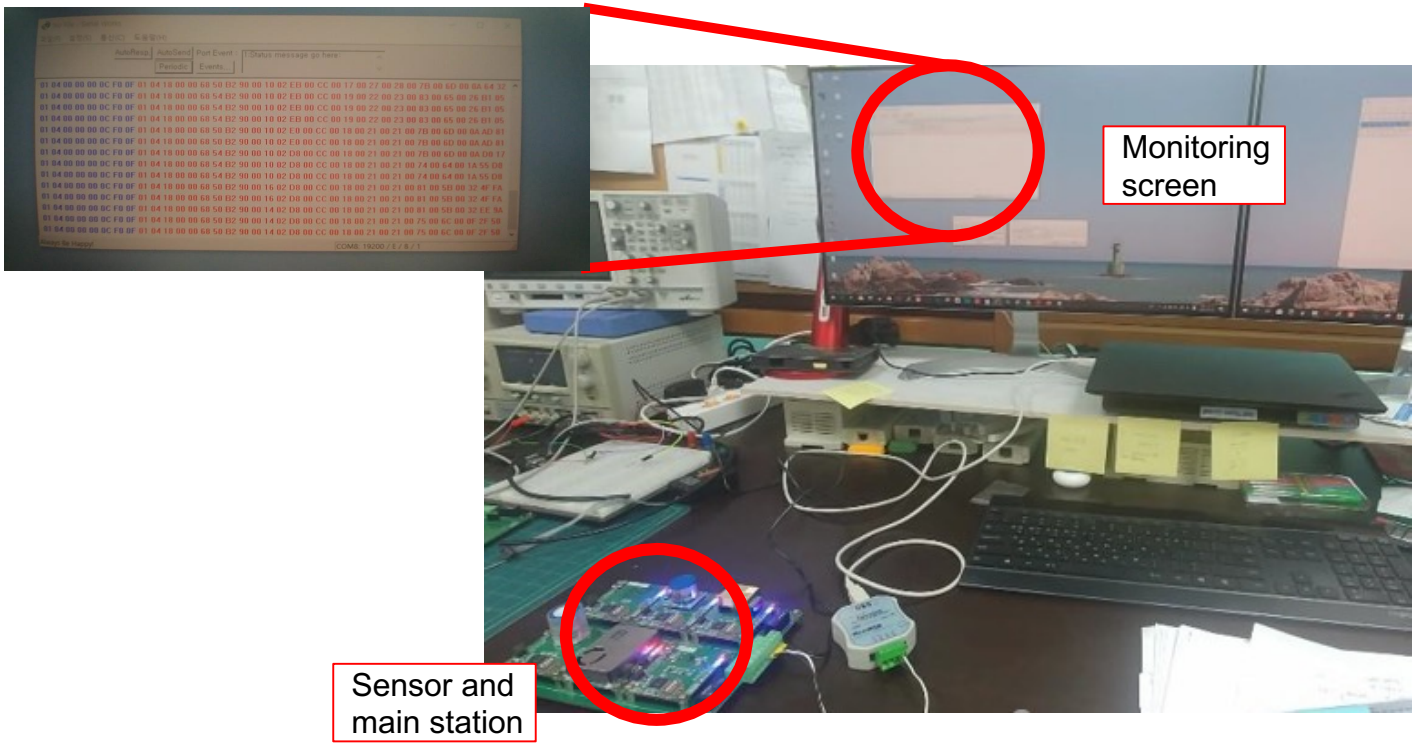

Figure. Testing the system

Part 4. Applied Technique

4.1 Existing Approaches for Fire Monitoring

- Multivariate statistical methods-based algorithms: Use sensor measurements fro m past time points
  - McAvoy et al. (1996) and Cestari et al. (2005)
    - Propose the usage of principle component analysis (PCA) to normal data
    - Use Q statistic for fire detection
  - JiJi et al. (2003)
    - Use Q and T^2-statistic with PCA for fire detection

  - Q-statistic: squared difference between the current and reconstructed (predicted) observation

$$Q = \left|\left|\boldsymbol{y}_{\text{new}} - \hat{\boldsymbol{y}}_{new}\right|\right|_2$$

$\boldsymbol{y}_{\text{new}}$: Current sensor observation
$\hat{\boldsymbol{y}}_{new}$: Reconstructed observation by using PCA

  - T^2-statistic: Distance between current and training observations based on Mahalanobis distan ce

$$T^2 = (\boldsymbol{z}_{\text{new}} - \boldsymbol{\mu}_{\text{Z}})\boldsymbol{\Sigma}_{\mathbf{Z}}(\boldsymbol{z}_{\text{new}} - \boldsymbol{\mu}_{\mathbf{Z}})^{\text{T}}$$

$\boldsymbol{z}_{\text{new}}$: Transformed observations of $\boldsymbol{y}_{\text{new}}$ by using PCA
$\boldsymbol{\mu}_{\text{Z}}$,$\boldsymbol{\Sigma}_{\mathbf{Z}}$: Mean and covariance of $\mathbf{Z}$ where $\mathbf{Z}$ is transformed training dataset by using PCA

- Drawbacks of multivariate statistical methods:
  - Consider each sensor measurement as a single feature
  - Fail to retain the temporal relationship among sensor signals while using PCA
  - PCA may not be useful in high-dimensional sensor data
    - PCA requires # of observations to be larger than # of features

4.1 Existing Approaches for Fire Monitoring

- Wavelet-based machine learning methods fire monitoring algorithms: Use sensor measurements from past time points
  - Wang et al. (2013)
    - Apply wavelet technique to denoise data
    - Artificial neural network (ANN) classification model in fire monitoring
  - Zheng et al. (2015)
    - Apply wavelet technique to denoise data
    - PCA is used to transformed data with reduced dimensions
    - Fuzzy RBF neural network is implemented

4.2 Challenging Issues in Fire Monitoring

- Fires types can be categorized as:
  - Flaming, smoldering and heating fire (cooking fire)

	Flaming	Heating	Smoldering
Temperature	Extremely High	Medium	Low
Flames	Visible	Invisible	Invisible

- Sensors react differently to fire types (KISTI data)
  - Flaming Fire
    - **O2 sensor reacts faster than dust sensor**
      - O2 should be present in air to generate flames
      - Lower concentration of smoke than smoldering type
  - Smoldering Fire:
    - **Dust sensor reacts faster than O2 sensor**
      - O2 is not necessary to generate smoldering fire
      - Higher concentration of smoke

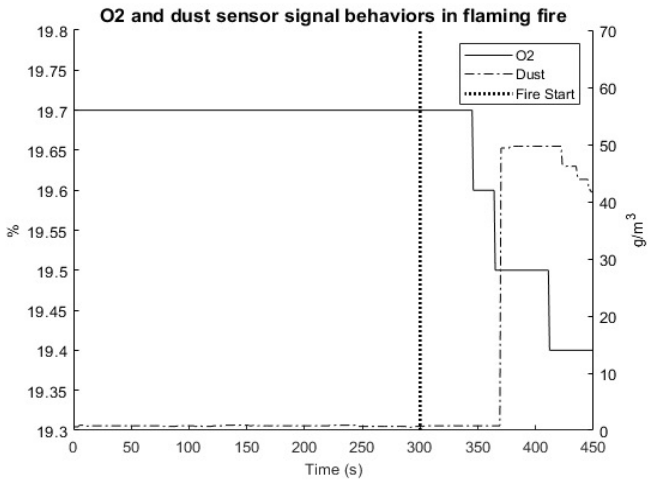

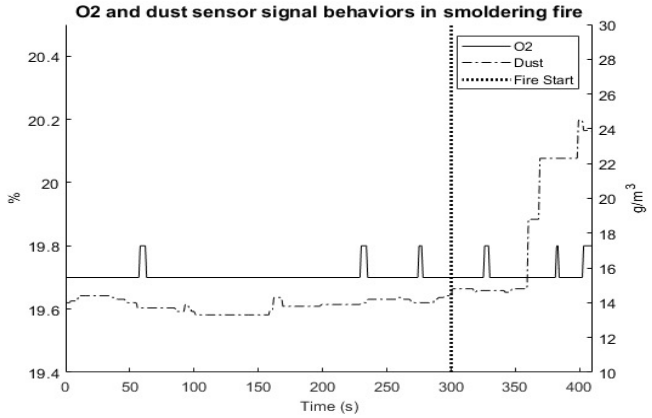

Figure. Sensor types react differently under different fire types

4.3 Objective and Contribution

- We propose a **wavelet-based real-time fire detection** system that combines Dynamic Time Warping distance measure.(WV-DTW)
  - Wavelet takes advantage of its multi-resolution property
  - Present new wavelet-based DTW similarity measure that can be useful in fi re monitoring
  - Allows time-distortion on Wavelet-based approach
  - Strengthen Wavelet-based weakness

.

4.4 Wavelet Based background

- Wavelet transform converts the signal in the time domain into an ap proximated data with two basis functions
  - Coarser wavelet: Represent the global and smooth parts of sensor signals
  - Finer wavelet: Represent the locality and details of the sensor signal

- By using the wavelet transform, original signal $f(t)$ can be approxima ted as following:

$$f(t) = \sum_{k=0}^{2^{L}-1} c_{L,k}\emptyset_{L,k}(t) + \sum_{j=L}^{J}\sum_{k=0}^{2^{L}-1} d_{j,k}\varphi_{j,k}(t)$$

coarser level *finer level*

$\emptyset_{L,k}(t)$: Coarser wavelet
$\varphi_{j,k}(t)$: Finer wavelets
$c_{L,k}$: Coefficient of coarser wavelet
$d_{j,k}$: Coefficient of finer wavelet

- Based on the changes of $c_{L,k}$ and $d_{j,k}$, various patterns of the fire sig nals can be captured

4.4 Wavelet Based background/ Haar Wavelets

- Haar's mother wavelet

$$\psi^{\text{Harr}}(x) = 1_{0 \le x < 1/2}(x) - 1_{1/2 \le x < 1}(x).$$

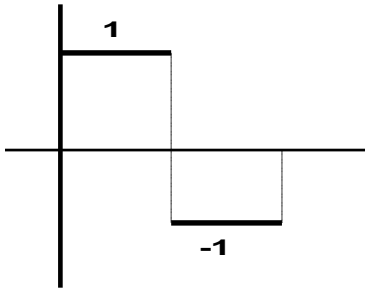

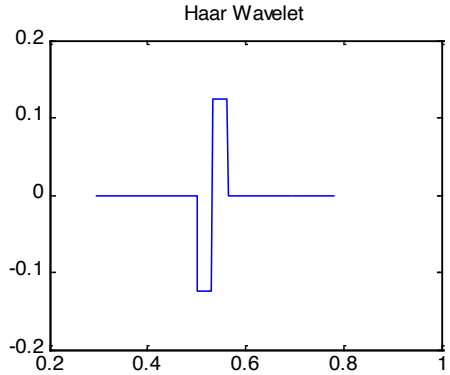

$$\psi(x) = \begin{cases} 1 & 0 \le x \le \frac{1}{2} \\ -1 & \frac{1}{2} < x \le 1 \\ 0 & \text{otherwise} \end{cases}$$

4.5 Scale Families of Haar Wavelets

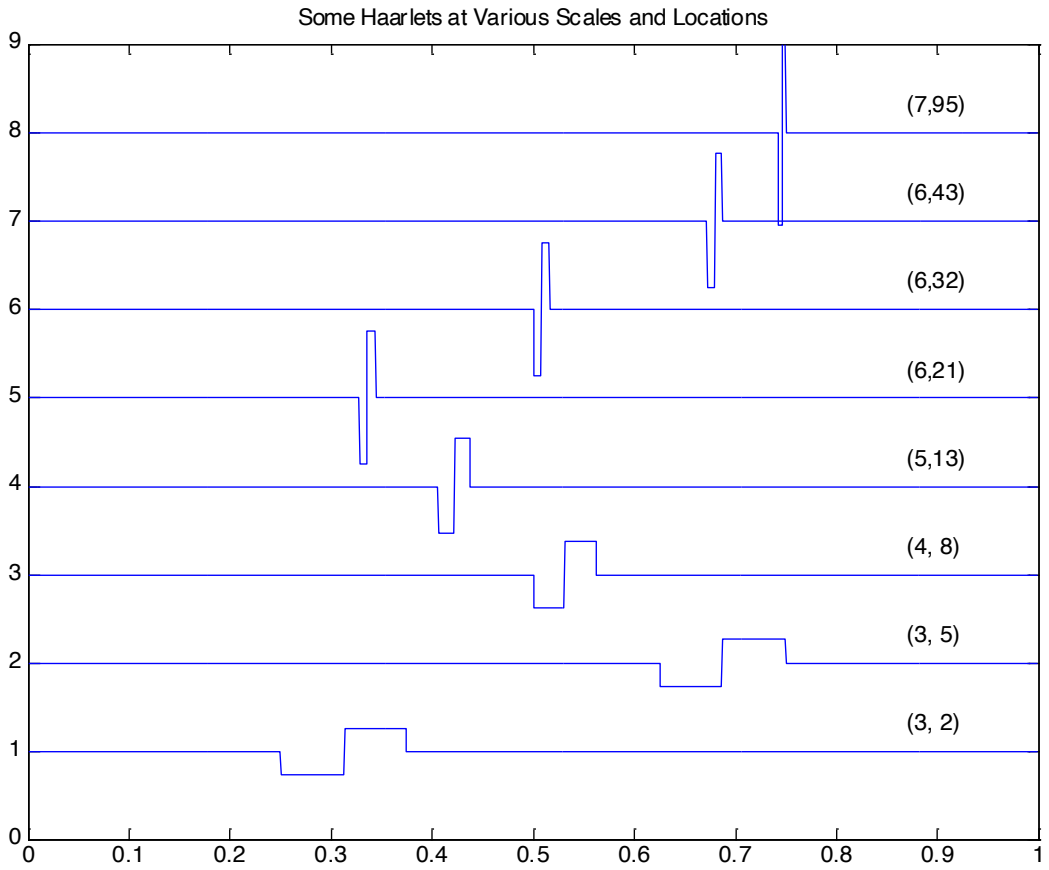

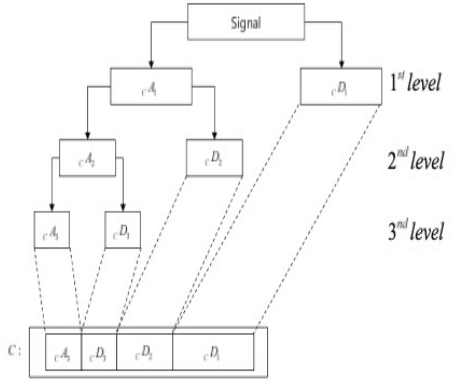

Coarse -> Finer level

4.5 Wavelet Based Multi-resolution Information

- At time point t, let sensor measurement of pth sensor $p \in \{1, \dots, P\}$ ar e available as follows:
  - $\boldsymbol{x}_p = \{x_p(t-31), x_p(t-30), \dots, x_p(t)\}$
  - Sensor measurements from current time t to past 31 points are available

- By applying discrete wavelet transform, we obtain (using the fifth-lev el Harr wavelet):

$$DWT[\boldsymbol{x}_p] = \begin{bmatrix} c^p_{4,1}, c^p_{4,2}, d^p_{4,1}, d^p_{4,2}, d^p_{3,1}, d^p_{3,2}, d^p_{3,3}, d^p_{3,4}, d^p_{2,1}, d^p_{2,2}, d^p_{2,3}, d^p_{2,4}, d^p_{2,5}, d^p_{2,6}, d^p_{2,7}, d^p_{2,8}, \\ d^p_{1,1}, d^p_{1,2}, d^p_{1,3}, d^p_{1,4}, d^p_{1,5}, d^p_{1,6}, d^p_{1,7}, d^p_{1,8}, d^p_{1,9}, d^p_{1,10}, d^p_{1,11}, d^p_{1,12}, d^p_{1,13}, d^p_{1,14}, d^p_{1,15}, d^p_{1,16} \end{bmatrix}$$

$c^p_{m,n}$ and $d^p_{m,n}$ are the n^{th} coarser and finer coefficients in scale m, respectively, f or p^{th} sensor signal

4.7 Wavelet Based Multi-resolution Information

- The equations of wavelet coefficients based on DWT

Feature vector	Wavelet coefficient formulation	Feature vector	Wavelet coefficient formulation
$s_{p,1}$	$c_{4,1}^{p} = \frac{1}{\sqrt{16}}\left(\sum_{j=16}^{31} x_p(t-j)\right)$	$s_{p,2}$	$c_{4,2}^{p} = \frac{1}{\sqrt{16}}\left(\sum_{j=0}^{15} x_p(t-j)\right)$
$s_{p,3}$	$d_{4,1}^{p} = \frac{1}{\sqrt{16}}\left(\sum_{j=31}^{23} x_p(t-j) - \sum_{t=16}^{22} x_p(t-j)\right)$	$s_{p,4}$	$d_{4,2}^{p} = \frac{1}{\sqrt{16}}\left(\sum_{j=8}^{15} x_p(t-j) - \sum_{t=0}^{7} x_p(t-j)\right)$
$s_{p,5}$	$d_{3,1}^{p} = \frac{1}{\sqrt{8}}\left(\sum_{j=28}^{31} x_p(t-j) - \sum_{j=24}^{27} x_p(t-j)\right)$	$s_{p,6}$	$d_{3,2}^{p} = \frac{1}{\sqrt{8}}\left(\sum_{j=20}^{23} x_p(t-j) - \sum_{j=16}^{19} x_p(t-j)\right)$
$s_{p,7}$	$d_{3,3}^{p} = \frac{1}{\sqrt{8}}\left(\sum_{j=12}^{15} x_p(t-j) - \sum_{j=8}^{11} x_p(t-j)\right)$	$s_{p,8}$	$d_{3,4}^{p} = \frac{1}{\sqrt{8}}\left(\sum_{j=4}^{7} x_p(t-j) - \sum_{j=0}^{3} x_p(t-j)\right)$
$s_{p,9}$	$d_{2,1}^{p} = \frac{1}{\sqrt{4}}\left(\sum_{j=30}^{31} x_p(t-j) - \sum_{j=28}^{29} x_p(t-j)\right)$	$s_{p,10}$	$d_{2,2}^{p} = \frac{1}{\sqrt{4}}\left(\sum_{j=26}^{27} x_p(t-j) - \sum_{j=24}^{25} x_p(t-j)\right)$
$s_{p,11}$	$d_{2,3}^{p} = \frac{1}{\sqrt{4}}\left(\sum_{j=22}^{23} x_p(t-j) - \sum_{j=20}^{21} x_p(t-j)\right)$	$s_{p,12}$	$d_{2,4}^{p} = \frac{1}{\sqrt{8}}\left(\sum_{j=18}^{19} x_p(t-j) - \sum_{j=16}^{17} x_p(t-j)\right)$
$s_{p,13}$	$d_{2,5}^{p} = \frac{1}{\sqrt{4}}\left(\sum_{j=14}^{15} x_p(t-j) - \sum_{j=12}^{13} x_p(t-j)\right)$	$s_{p,14}$	$d_{2,6}^{p} = \frac{1}{\sqrt{4}}\left(\sum_{j=10}^{11} x_p(t-j) - \sum_{j=8}^{9} x_p(t-j)\right)$
$s_{p,15}$	$d_{2,7}^{p} = \frac{1}{\sqrt{4}}\left(\sum_{j=6}^{7} x_p(t-j) - \sum_{j=4}^{5} x_p(t-j)\right)$	$s_{p,16}$	$d_{2,8}^{p} = \frac{1}{\sqrt{4}}\left(\sum_{j=2}^{3} x_p(t-j) - \sum_{j=0}^{1} x_p(t-j)\right)$
$s_{p,17}$	$d_{1,1}^{p} = \frac{1}{\sqrt{2}}\left(x_p(t-31) - x_p(t-30)\right)$	$s_{p,18}$	$d_{1,2}^{p} = \frac{1}{\sqrt{2}}\left(x_p(t-29) - x_p(t-28)\right)$
$s_{p,19}$	$d_{1,3}^{p} = \frac{1}{\sqrt{2}}\left(x_p(t-27) - x_p(t-26)\right)$	$s_{p,20}$	$d_{1,4}^{p} = \frac{1}{\sqrt{2}}\left(x_p(t-25) - x_p(t-24)\right)$
$s_{p,21}$	$d_{1,5}^{p} = \frac{1}{\sqrt{2}}\left(x_p(t-23) - x_p(t-22)\right)$	$s_{p,22}$	$d_{1,6}^{p} = \frac{1}{\sqrt{2}}\left(x_p(t-21) - x_p(t-20)\right)$
$s_{p,23}$	$d_{1,7}^{p} = \frac{1}{\sqrt{2}}\left(x_p(t-19) - x_p(t-18)\right)$	$s_{p,24}$	$d_{1,8}^{p} = \frac{1}{\sqrt{2}}\left(x_p(t-17) - x_p(t-16)\right)$
$s_{p,25}$	$d_{1,9}^{p} = \frac{1}{\sqrt{2}}\left(x_p(t-15) - x_p(t-14)\right)$	$s_{p,26}$	$d_{1,10}^{p} = \frac{1}{\sqrt{2}}\left(x_p(t-13) - x_p(t-12)\right)$
$s_{p,27}$	$d_{1,11}^{p} = \frac{1}{\sqrt{2}}\left(x_p(t-11) - x_p(t-10)\right)$	$s_{p,28}$	$d_{1,12}^{p} = \frac{1}{\sqrt{2}}\left(x_p(t-9) - x_p(t-8)\right)$
$s_{p,29}$	$d_{1,13}^{p} = \frac{1}{\sqrt{2}}\left(x_p(t-7) - x_p(t-6)\right)$	$s_{p,30}$	$d_{1,14}^{p} = \frac{1}{\sqrt{2}}\left(x_p(t-5) - x_p(t-4)\right)$
$s_{p,31}$	$d_{1,15}^{p} = \frac{1}{\sqrt{2}}\left(x_p(t-3) - x_p(t-2)\right)$	$s_{p,32}$	$d_{1,16}^{p} = \frac{1}{\sqrt{2}}\left(x_p(t-1) - x_p(t)\right)$

4.7 Wavelet Based Multi-resolution Information

- Different types of fire can be effectively detected from wavelet coeffic ients
  - Finer coefficients
    - Sharp and abrupt changes can be effectively detected
    - Flaming fire
  - The coarser coefficients:

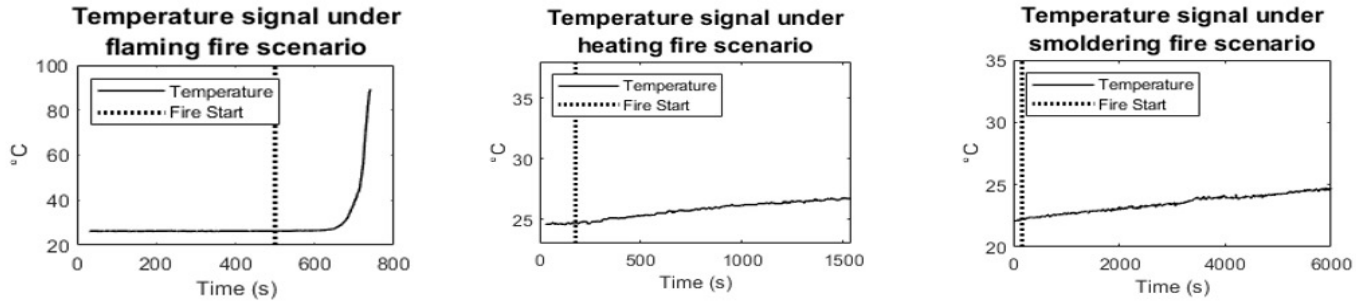

Figure. Raw sensor signals

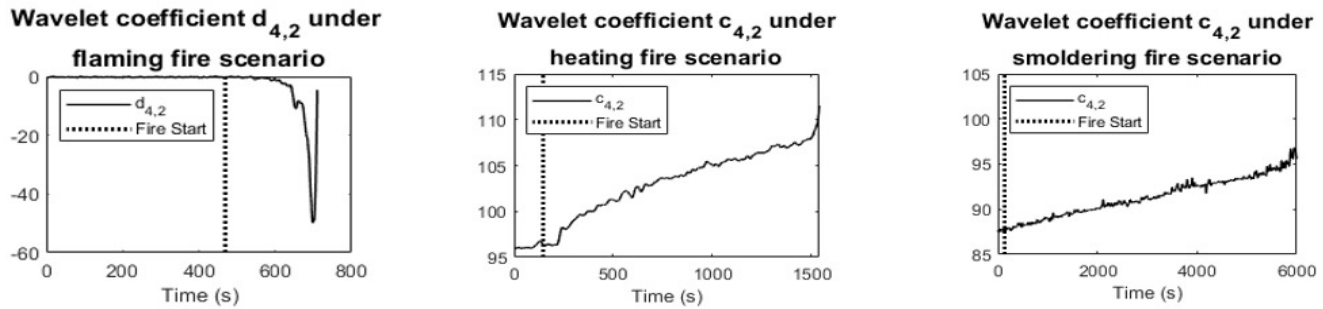

Figure. Wavelet coefficients

Dynamic Time Warping

4.8 Dynamic Time Warping Background

- Considers multichannel sensor signals from both current and past me asurements from multiple locations

- Develops a fire detection method based on Dynamic Time Warping (DTW) as a time series similarity measures
  - DTW allows preserving temporal dynamics in the sensor signals
  - Non-linear alignment matching of DTW allows capturing complicated patterns and shape of signal in different fire types

- Develop the k-out-of-P: fire voting rule
  - Sensors react differently based on the **fire type** and the **sensor location**
  - Combines decision rules from P multichannel sensor signals
  - Adaptively combines essential sensors that react faster

4.9 DTW Objective and Contribution

- Considers multichannel sensor signals from both current and past me asurements from multiple locations

- Develops a fire detection method based on Dynamic Time Warping (DTW) as a time series similarity measures
  - DTW allows preserving temporal dynamics in the sensor signals
  - Non-linear alignment matching of DTW allows capturing complicated patterns and shape of signal in different fire types

4.10 Time Series Similarity Measures: Euclidean Distance

- Let $\boldsymbol{x}_1 = \{x_1(i) \in \mathbb{R}: i = 1, \ldots, T\}$ and $\boldsymbol{x}_2 = \{x_2(j) \in \mathbb{R}: j = 1, \ldots, T\}, T$ is a length of the sensor signals, $\boldsymbol{x}_1$ and $\boldsymbol{x}_2$

- Euclidean Distance
  - $ED(\boldsymbol{x}_1, \boldsymbol{x}_2) = \sqrt{\sum_{i=1}^{T}\left(x_1(i) - x_2(i)\right)^2}$
  - Linear alignment

- Drawback of ED
  - ED measure is very sensitive when time distortion exists in $\boldsymbol{x}_1$ and $\boldsymbol{x}_2$
    - The distance increases with presence of the time distortion even when the two sequences are under the same process.

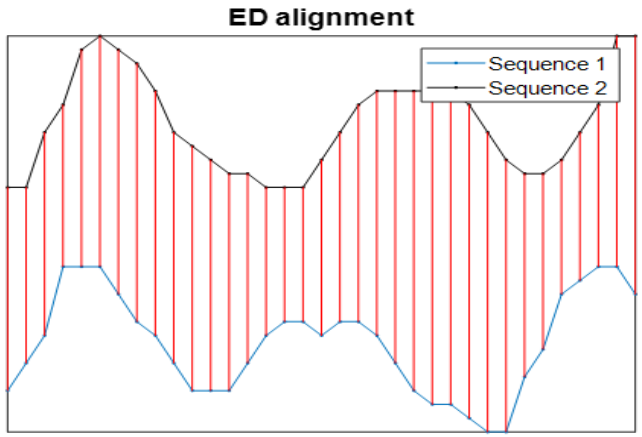

Figure. Alignment result between two sequences by using ED

- Dynamic time warping
  - A nonlinear mapping technique
  - Evaluate similarities in a more flexible m anner
  - $DTW(\boldsymbol{x}_1, \boldsymbol{x}_2) = min \frac{1}{K} \sqrt{\sum_{k=1}^{K} d_l\left(x_1(i_k), x_2(j_k)\right)}$
    - $\Gamma(i,j) = d\left(x_1(i), x_2(j)\right) + \min \begin{cases} \Gamma(i-1, j-1) \\ \Gamma(i-1, j) \\ \Gamma(i, j-1) \end{cases}$

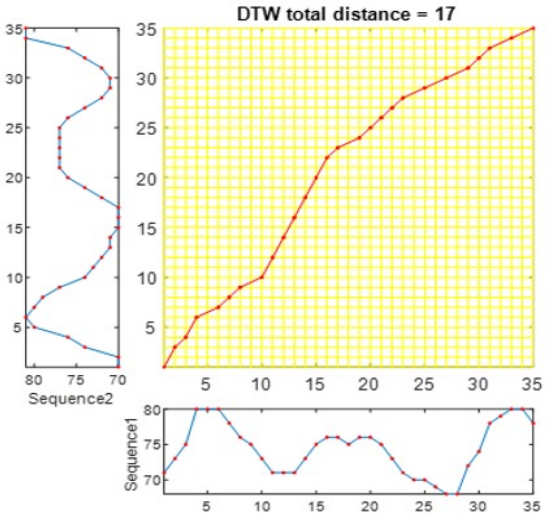

Figure. Warping matrix and optimal w arping path by DTW

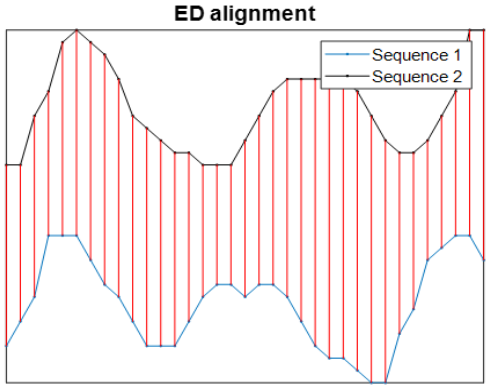

Figure. Alignment result between two seq uences by using ED

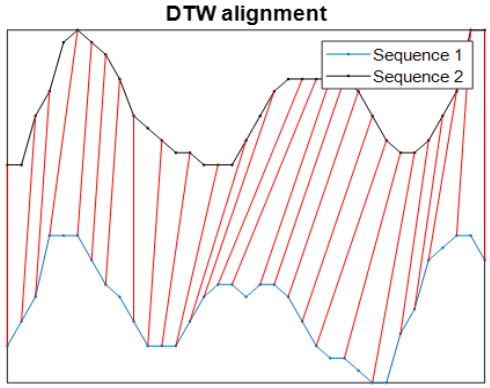

Figure. Alignment result between two seq uences by using DTW

It allows Time-distortion

4.11 Time Series Similarity Measures: Dynamic Time Warping (DTW)

- Similarity among fire sensor measurements from different time points can be effectively evaluated by DTW
  - Alignment of two normal situation signals using DTW
    - Two sequences are not exactly the same
    - Point in the black sequence is matched with nearer neighbors of the blue sequence

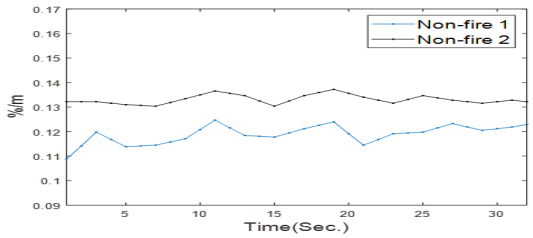

Figure. Raw signals

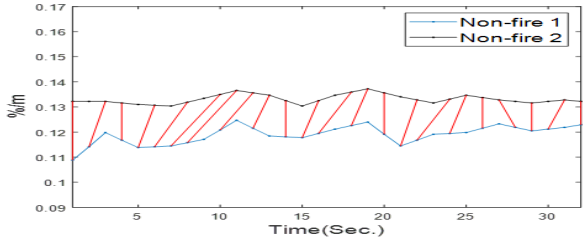

Figure. DTW alignment

  - Alignment of a normal situation signal and a fire situation signal using DTW
    - DTW maps a point from the black sequence to the blue sequence with the further distance due to two distinct sequence patterns

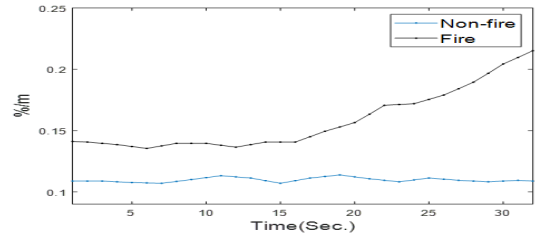

Figure. Raw signals

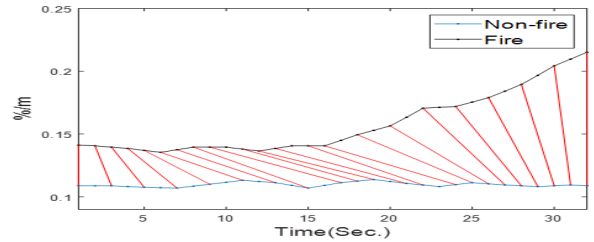

Figure. DTW alignment

4.12 WV-DTW Similarity Measure

- Algorithm Steps

  Suppose that we have

  - $\boldsymbol{x_1} = \{\boldsymbol{x}_1(\boldsymbol{i}), \in R: \boldsymbol{i} = \boldsymbol{1}, \ldots, \boldsymbol{T}\}$, $\boldsymbol{x_2} = \{\boldsymbol{x}_2(\boldsymbol{i}), \in R: \boldsymbol{i} = \boldsymbol{1}, \ldots, \boldsymbol{T}\}$ where T is a length of the sensor signals
  - Obtain warping path, $W = \boldsymbol{w}_1, w_2, \ldots, w_k, \ldots, w_K$ from DTW where $w_k = (i_k, j_k)$ r epresents index i of x_1 and index x_2 in the k-th warping path of W. $K$is the len gth of warping path.
  - Optimal warping path path can be obtained by minimizing the warping cost defined as follows $DTW = \min \frac{1}{K} \left\{ \sqrt{\sum_{k=1}^{K} d_1(x_1(i_k), \boldsymbol{x_2}(\boldsymbol{j_k}))} \right\}$
  - **Construct new alignment path where the component** of $\boldsymbol{x_1'} = \{\boldsymbol{x_1}(\boldsymbol{i_1}), \boldsymbol{x_1}(\boldsymbol{i_2}), \ldots, \boldsymbol{x_1}(\boldsymbol{i_k})\}$ and $\boldsymbol{x_2'} = \{\boldsymbol{x_2}(\boldsymbol{i_1}), \boldsymbol{x_2}(\boldsymbol{i_2}), \ldots, \boldsymbol{x_2}(\boldsymbol{i_k})$.

4.12 WV-DTW Similarity Measure

- Obtain wavelet coefficient by using DWT $DWT[\boldsymbol{x}'_1]$ and $DWT[\boldsymbol{x}'_2]$ from $\boldsymbol{x}'_1$ *and* $\boldsymbol{x}'_2$. Harr. Wavelet is applied, its DWT can be expressed as

$$DWT[\boldsymbol{x}'_1] = \begin{bmatrix} c^1_{4,1}, c^1_{4,2}, d^1_{4,1}, d^1_{4,2}, d^1_{3,1}, d^1_{3,2}, d^1_{3,3}, d^1_{3,4}, d^1_{2,1}, d^1_{2,2}, d^1_{2,3}, d^1_{2,4}, d^1_{2,5}, d^1_{2,6}, d^1_{2,7}, d^1_{2,8}, \\ d^1_{1,1}, d^1_{1,2}, d^1_{1,3}, d^1_{1,4}, d^1_{1,5}, d^1_{1,6}, d^1_{1,7}, d^1_{1,8}, d^1_{1,9}, d^1_{1,10}, d^1_{1,11}, d^1_{1,12}, d^1_{1,13}, d^1_{1,14}, d^1_{1,15}, d^1_{1,16} \end{bmatrix}$$

$$DWT[\boldsymbol{x}'_2] = \begin{bmatrix} c^2_{4,1}, c^2_{4,2}, d^2_{4,1}, d^2_{4,2}, d^2_{3,1}, d^2_{3,2}, d^2_{3,3}, d^2_{3,4}, d^2_{2,1}, d^2_{2,2}, d^2_{2,3}, d^2_{2,4}, d^2_{2,5}, d^2_{2,6}, d^2_{2,7}, d^2_{2,8}, \\ d^2_{1,1}, d^2_{1,2}, d^2_{1,3}, d^2_{1,4}, d^2_{1,5}, d^2_{1,6}, d^2_{1,7}, d^2_{1,8}, d^2_{1,9}, d^2_{1,10}, d^2_{1,11}, d^2_{1,12}, d^2_{1,13}, d^2_{1,14}, d^2_{1,15}, d^2_{1,16} \end{bmatrix}$$

where $c^p_{m,n}$ and $d^p_{m,n}$ are n^{th} coarser and finer coefficients in scale m.

- The Euclidean distance between two signals, $\boldsymbol{x}'_1$ and $\boldsymbol{x}'_2$, can be defined as:

$$WVDTW\ ED(\boldsymbol{x}'_1, \boldsymbol{x}'_2) = \sqrt{\sum_{i=1}^{T} DWT\left((\boldsymbol{x}'_1(i)) - DWT(\boldsymbol{x}'_2(i)\right)^2}$$

4.13 WV-DTW Similarity Measure

- WV-DTWNN Real time fire detection algorithm observation window

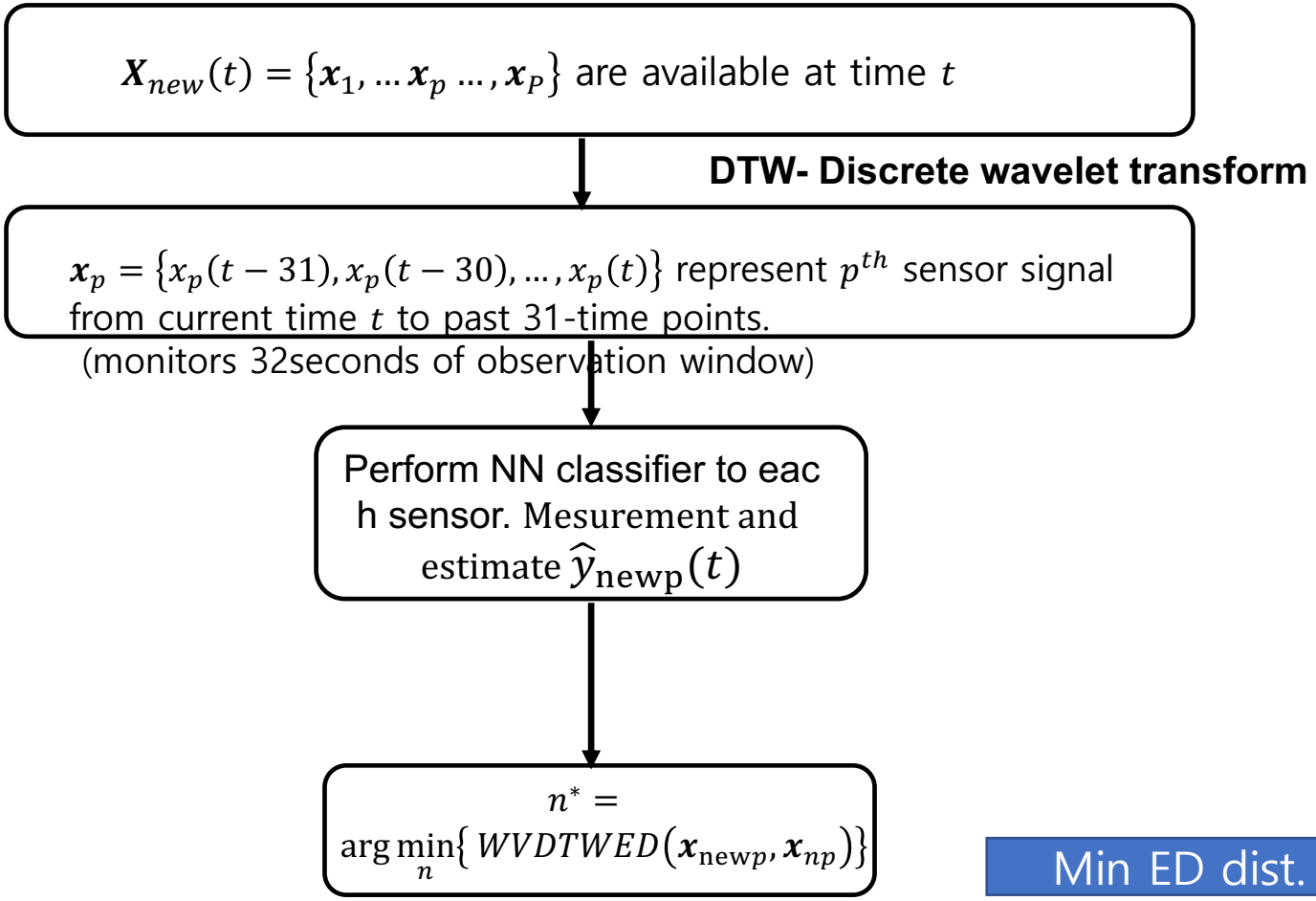

4.13 Real-Time Fire Detection System

- Some sensors react late to fire based on the fire type and the sensor location

- "k-out-of-P: fire voting rule"
  - Integrate the labels of each sensor $\hat{y}_{\mathrm{new}p}$ to predict the final label $\hat{y}_{\mathrm{new}}$
  - Adaptively combines essential sensors that react faster than others
  - Classify $\boldsymbol{X}_{\mathrm{new}}$ as
    - "fire" (i.e., $\hat{y}_{\mathrm{new}} = 1$) when $\sum_{p=1}^{P} \hat{y}_{\mathrm{new}p} \geq k$
    - Otherwise $\boldsymbol{X}_{\mathrm{new}}$ is classified as "non-fire" (i.e., $\hat{y}_{\mathrm{new}} = 0$)

Part 5 :
Results and Analysis

5.1 Case Study : Performance Measure

- Performance measure
  - Fire starting time accuracy (FSTA): $FSTA = |TFST - EFST|$
    - $TFST$ is the true fire starting time
    - $EFST$ is the estimated fire starting time obtained by the fire detection algorithm for a giv en scenario

  - False alarm rate (FAR): $FAR = \left[\frac{1}{TFST-1} * \sum_{t=1}^{TFST-1} |\hat{y}(t) - y(t)|\right]$
    - $y(t) \in \{0, 1\}$ is a true fire label at time t
    - $\hat{y}(t) \in \{0, 1\}$ is the predicted fire label at time t.

5.1 Case Study : Performance Comparison

- Performance comparison

Scenario #	TFST	TBA 1			Q-statistic			T^2-statistic		
		EFST (sec)	FSTA (sec)	FAR (%)	EFST (sec)	FSTA (sec)	FAR (%)	EFST (sec)	FSTA (sec)	FAR (%)
1	967	4310	3343	0.21	4330	3363	0.00	365	602	5.02
2	678	2105	1427	0.74	2114	1436	0.00	2254	1576	0.00
3	1000	2225	1225	2.4	2341	1341	0.00	2342	1342	0.00
4	1000	1085	85	0	1167	167	0.00	1192	192	0.00
5	1000	1129	129	2.5	1177	177	0.00	1216	216	0.00
6	1000	736	264	3.7	1176	176	0.00	1222	222	0.00
7	738	819	81	0	823	85	0.00	40	698	37.48
8	1000	1069	69	8.91	215	785	72.96	1115	115	0.00
9	1000	1063	63	3.6	1071	71	0.00	1103	103	0.00
10	1000	1067	67	5.61	1092	92	0.00	1129	129	0.00
Average	967	4310	3343	0.21		769.30	7.30		519.50	4.25
(std)			(1068.00)	(2.86)		(1052.99)	(23.07)		(538.40)	(11.78)
Scenario #	TFST	PNN			NN-ED			NN-DTW		
		EFST (sec)	FSTA (sec)	FAR (%)	EFST (sec)	FSTA (sec)	FAR (%)	EFST (sec)	FSTA (sec)	FAR (%)
1	967	4320	3353	0.00	1944	977	0.00	**1941**	974	0.00
2	678	1977	1299	0.00	953	275	0.00	**949**	271	0.00
3	1000	1883	883	0.00	1704	704	0.00	**1703**	703	0.00
4	1000	1166	166	0.00	1098	98	0.00	**1089**	89	0.00
5	1000	1207	207	0.00	1114	114	0.00	**1113**	113	0.00
6	1000	1213	213	0.00	1125	125	0.00	**1124**	124	0.00
7	738	817	79	0.00	783	45	0.00	**782**	44	0.00
8	1000	1163	163	0.00	1055	55	0.00	**1052**	52	0.00
9	1000	1119	119	0.00	1070	70	0.00	**1068**	68	0.00
10	1000	1132	132	0.00	1103	103	0.00	**1102**	102	0.00
Average			661.40	0.00		256.60	0.00		**254.00**	**0.00**
(std)			(1028.23)	(0.00)		(320.78)	(0.00)		(320.92)	(0.00)

5.1 Case Study : Performance Comparison

- Performance comparison

NN-DTW		
EFST (sec)	FSTA (sec)	FAR (%)
1941	974	0.00
949	271	0.00
1703	703	0.00
1089	89	0.00
1113	113	0.00
1124	124	0.00
782	44	0.00
1052	52	0.00
1068	68	0.00
1102	102	0.00
	254.00	**0.00**
	(320.92)	(0.00)

WV-DTW		
EFST (sec)	FSTA (sec)	FAR (%)
410	117	0.00
44	259	7.00
377	74	0.00
371	77	0.00
658	358	0.00
347	47	0.00
377	77	0.00
486	186	0.00
505	205	0.00
417	117	0.74
41	**140.55**	**0.55**
	(148)	(0.00)

WV-DTW is better than DTW
in FSTA(Fire Starting Time Accuracy) but not significantly higher FAR

5.2 Case Study : Performance Comparison

- Performance analysis
  - Thresholding based algorithms (TBA)
    - TBAs detect a fire before the fire ignition and result in high false alarm rates
  - Q-statistic, T^2-statistic
    - Temporal information that exists in sensor signals is lost from using PCA
  - PNN
    - Consider each sensor measurement as a feature
    - Loss of temporal relationships between time points
  - DTW-NN
    - Obtain the best EFST and allows a robust performance regardless of fire types
    - Shows better performance than ED distance in the fire monitoring system
      - DTW allows non-linear alignment between two sensor signals
      - DTW captures complex patterns and shapes of sensor signals in different fire types
  - WV-DTW
    - Shows. better performance than DTW or existing method
    - Includes DTW traits and

5.3 Conclusions and Suggestions

- In this study, we developed a real-time fire detection system based on time series similarity measures for automated fire detection system based on **new similarity measure and sensor-board communication.**
- We adopted the new time series distance measure (WV-DTW) to evaluate similar patterns among complex sensor signals
- We proposed the k-out-of-P: fire voting classifier to adaptively choose sensors that are most relevant for detecting a fire
- We found that the proposed approach performs better than other existing approaches in terms of obtaining low EFST but slightly higher FAR.
- To reduce error rate, we could suggest Weighted DTW combined with Wavelet methods.